Journal of Geophysical Research - Biogeosciences

Supporting Information for

Varying contributions of drivers to the relationship between canopy photosynthesis and far-red sun-induced fluorescence for two maize sites at different temporal scales

Guofang Miao[1,*], Kaiyu Guan[1,2,*], Andrew E. Suyker[3], Xi Yang[4], Timothy J. Arkebauer[5], Elizabeth A. Walter-Shea[3], Hyungsuk Kimm[1], Gabriel Y. Hmimina[3], John A. Gamon[3,6], Trenton E. Franz[3], Christian Frankenberg[7,8], Joseph A. Berry[9], and Genghong Wu[1]

1. Department of Natural Resources and Environmental Sciences, University of Illinois at Urbana-Champaign, Urbana, IL, USA
2. National Center of Supercomputing Applications, University of Illinois at Urbana-Champaign, Urbana, IL, USA
3. School of Natural Resources, University of Nebraska-Lincoln, Lincoln, NE, USA
4. Department of Environmental Sciences, University of Virginia, Charlottesville, VA, USA
5. Department of Agronomy and Horticulture, University of Nebraska-Lincoln, Lincoln, NE, USA
6. University of Alberta, Departments of Earth & Atmospheric Sciences and Biological Sciences, Edmonton, AB, CAN
7. Division of Geological and Planetary Sciences, California Institute of Technology, Pasadena, CA, USA
8. NASA Jet Propulsion Laboratory, California Institute of Technology, Pasadena, CA, USA
9. Department of Global Ecology, Carnegie Institution of Washington, Stanford, CA, USA

Contents of this file

Introduction

This supporting file provides:

- The detailed description of the relative importance method (i.e. the Lindeman-Merenda-Gold method, Text S1).
- F_{760} unit conversion (Text S2).
- Seasonal variations of environmental drivers including air temperature, vapor pressure deficit, and precipitation (Figure S1).
- Seasonal variations of canopy leaf area index and canopy height (Figure S2).
- Two images (Figure S2) showing the field view of the instruments and one maize site (Figure S3).
- The contribution analysis result with fPAR at R4-R5 stages replaced by $fPAR_{green}$ that were derived from the normalized Red Edge Index (Figure S4).
- The identification of the growth stages of the two study sites (Table S1).
- Additional regression coefficients of the relationships between APAR and GPP, F_{760}, LUE, and F_{760} yield (Table S2).

Text S1: The Lindeman-Merenda-Gold (LMG) method (Grömping, 2007)

For a linear regression model (Equation S1)

$$Y_i = \beta_0 + \beta_1 X_{1,i} + \ldots + \beta_p X_{p,i} + \varepsilon \quad \text{(S1)}$$

in which the random variables X_j, j = 1, 2,..., p, represents p regressor variables and ε represents a random error term, $\varepsilon \sim N\left(0, \sigma^2\right)$, which is independent of other regressors. The coefficient of determination (R^2) of the regression model, which measures the proportion of variation in Y that is explained by the p regressors in the linear model, is calculated as Equation S2.

$$R^2 = \frac{\text{Model SS}}{\text{Total SS}} = \frac{\sum_i \left(Y_i - \overline{Y}\right)^2}{\sum_i \left(Y_i - \overline{Y}\right)^2} \quad \text{(S2)}$$

The relative contribution of the X_j regressor variable is then defined as the proportion of R^2 that is explained by X_j. To decompose the R^2 for the case that the p regressors are correlated, the LMD method uses sequential R^2s and takes the dependence on orderings into account by averaging the sequential R^2 over orderings (Equation S3). In Equation S3, LMG(X_k) is the relative contribution of X_k to the variation in Y; S represents a regressor set excluding X_k, and n(S) is the number of regressor in S; $seqR^2\left(\{X_k\}|S\right)$ is the additional R^2 when adding X_k to the regressor set S; $R^2\left(\{X_k\} \cup S\right)$ is the R^2 of the regression including both X_k and S; R^2(S) is the R^2 of the regression with only regressor set S included.

$$\begin{cases} seqR^2\left(\{X_k\} \mid S\right) = R^2\left(\{X_k\} \cup S\right) - R^2\left(S\right) \\ LMG\left(X_k\right) = \dfrac{1}{p!} \displaystyle\sum_{S \subseteq \{X_1, X_2, \ldots, X_p\} \setminus \{X_k\}} n\left(S\right)!\left(p - n\left(S\right) - 1\right)! seqR^2\left(\{X_k\}|S\right) \end{cases} \quad \text{(S3)}$$

Applying Eq. S3 to the LUE model, Y = ln(GPP), p = 3, X_1 =ln(PAR), X_2 = ln(fPAR), X_3 = ln(LUE), we can then calculate the relative contribution of each variable in the LUE models to the variations in

GPP or SIF. For example, the relative contribution of LUE to GPP can be calculated as follows (Equation S4):

$$\begin{cases} n(S)=0,\ S=\{\ \} \\ n(S)=1,\ S=\{X_1\} \text{ or } S=\{X_2\} \\ n(S)=2,\ S=\{X_1,X_2\} \\ LMG(X_3)=\frac{1}{3!}\sum_S n(S)!\left(2-n(S)\right)!seqR^2\left(\{X_3\}\,|\,S\right) \end{cases} \quad \text{(S4)}$$

Text S2: F_{760} unit conversion

The energy of 1 photon (E_p) is calculated as follows:

$$\begin{aligned} E_p &= \frac{hc}{\lambda} = \frac{6.63\times10^{-34}\left(J\ s\right)\times 2.998\times10^{8}\left(m\ s^{-1}\right)}{760\left(nm\right)} \\ &= 2.62\times10^{-19}\ J\ = 2.62\times10^{-16}\ \left(mW\ s\right) \end{aligned} \quad \text{(S5)}$$

in which h is the Planck Constant, c is the speed of light, and λ is wavelength. In the brackets is the unit of each variable. Accordingly, the energy of 1 μmol photons (E) is calculated as follows:

$$\begin{aligned} E &= \frac{6.02\times10^{23}\left(mol^{-1}\right)}{10^{6}\left(\mu mol\ mol^{-1}\right)}\times E_p\left(mW\ s\right) \\ &= 157.7\ mW\ s\ \mu mol^{-1} \end{aligned} \quad \text{(S6)}$$

We then converted the energy-based F_{760} (mW m^{-2} nm^{-1} sr^{-1}) to the photon flux-based F_{760} (μmol photons at 760 nm m^{-2} s^{-1} nm^{-1} sr^{-1}):

$$\begin{aligned} F_{760}\left(\mu mol\ m^{-2}\ s^{-1}\ nm^{-1}\ sr^{-1}\right) &= \frac{F_{760}\left(mW\ m^{-2}\ nm^{-1}\ sr^{-1}\right)}{E\left(mW\ s\ \mu mol^{-1}\right)} \\ &= F_{760}\left(mW\ m^{-2}\ nm^{-1}\ sr^{-1}\right)\times 0.0063\left(\frac{1}{mW\ s\ \mu mol^{-1}}\right) \end{aligned} \quad \text{(S7)}$$

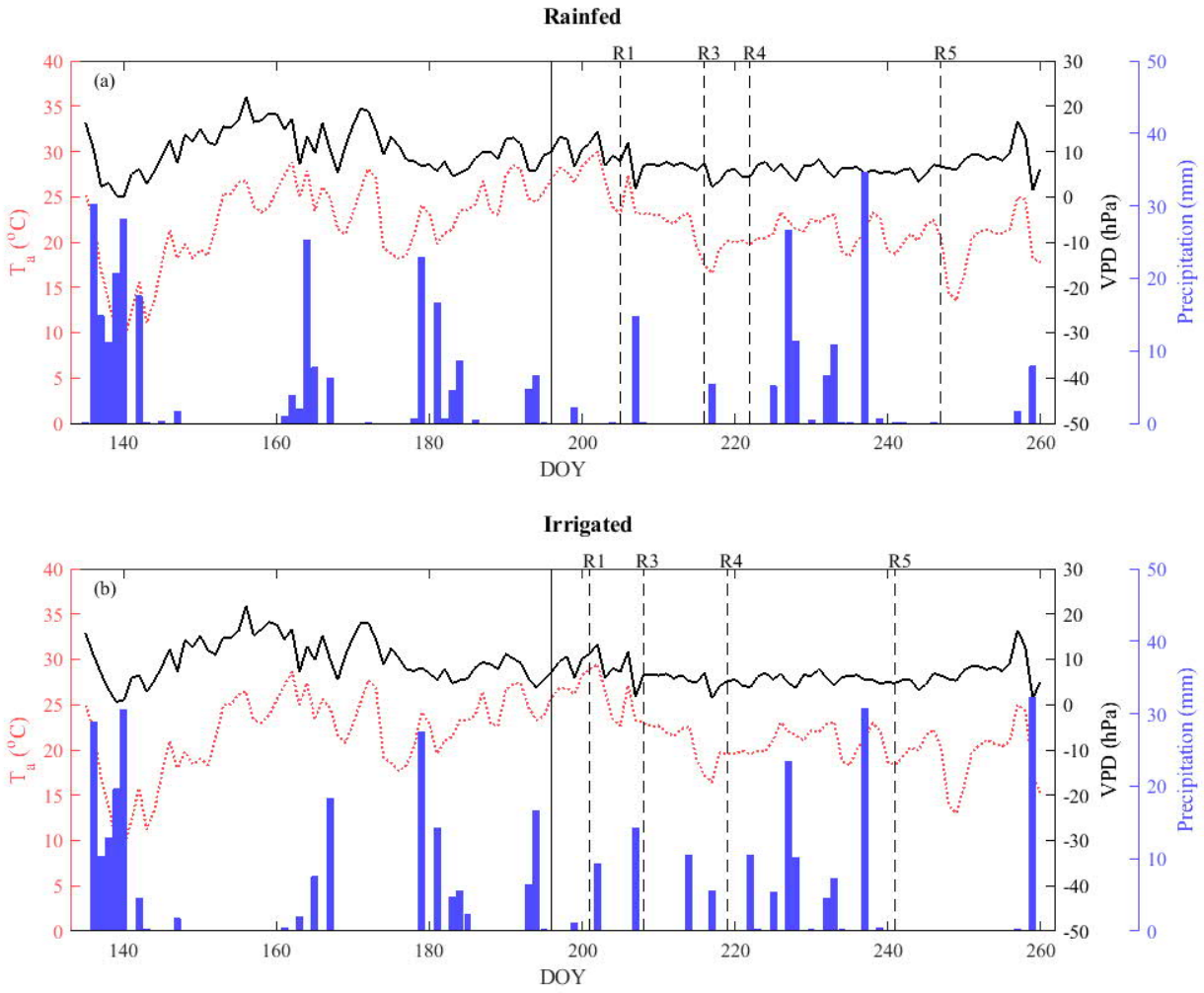

Figure S1. (a) Time series of air temperature (dotted red line), vapor pressure deficit (VPD, soild black line), and precipitation (blue bar) from May 15 to September 17, 2017 (DOY 135 - 260) at (a) the rainfed (US-Ne3) and (b) the irrigated (US-Ne2) maize site at Mead, Nebraska. The solid vertical black lines marked the starting date of the study period (DOY 196). The dashed vertical black lines marked the approximate starting dates of four growth stages recorded from selected plants - R1 (silking), R3 (milk), R4 (Dough), and R5 (Dent).

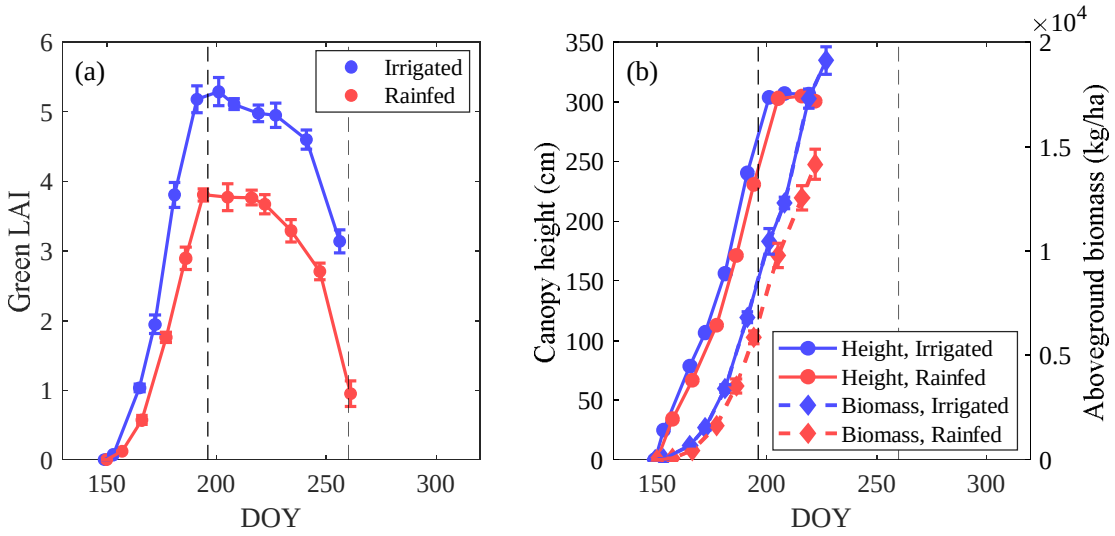

Figure S2. Time series of (a) green LAI, (b) canopy height and aboveground biomass at the rainfed (US-Ne3) and the irrigated (US-Ne2) maize site at Mead, Nebraska. Dashed lines marked the starting and the end of the dates of the study period (DOY 196 – 260).

(a)

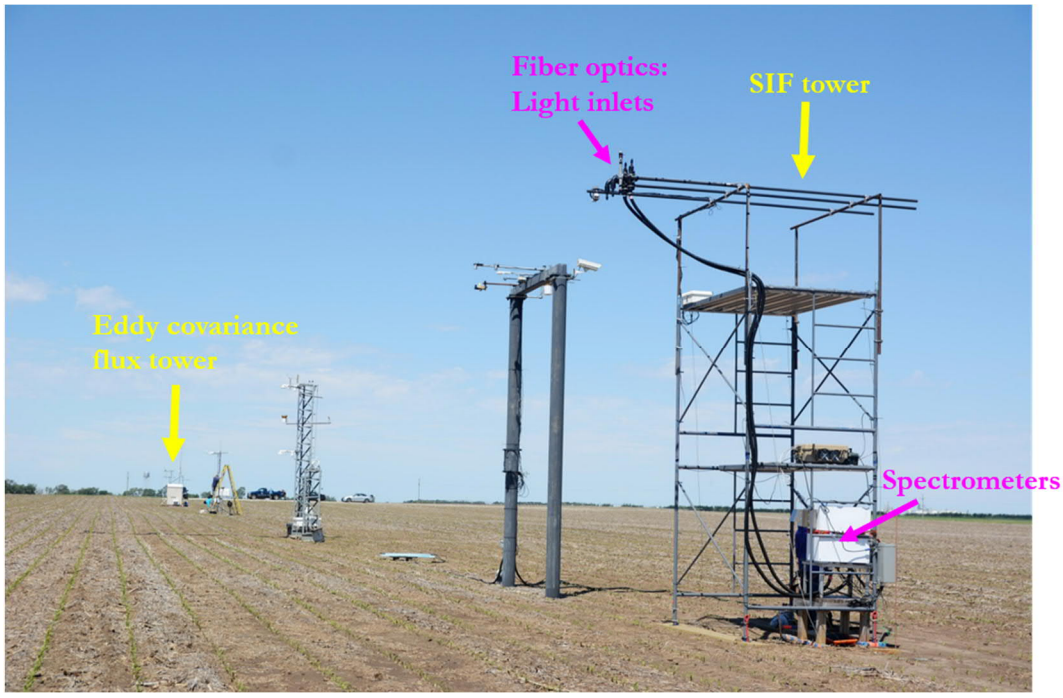

(b)

Figure S3. (a) Field instrument array at the rainfed maize site in Mead, Nebraska. The photo was taken when the SIF tower was first established in May 2017. The SIF towers and Fluospec2 systems at both rainfed and irrigated maize sites were damaged by a wind storm in June 2017. Re-establishment was finished in July 2017 and SIF measurements restarted on July 14, 2017. (b) The rainfed maize site at vegetative tasseling stage (July 19, 2017).

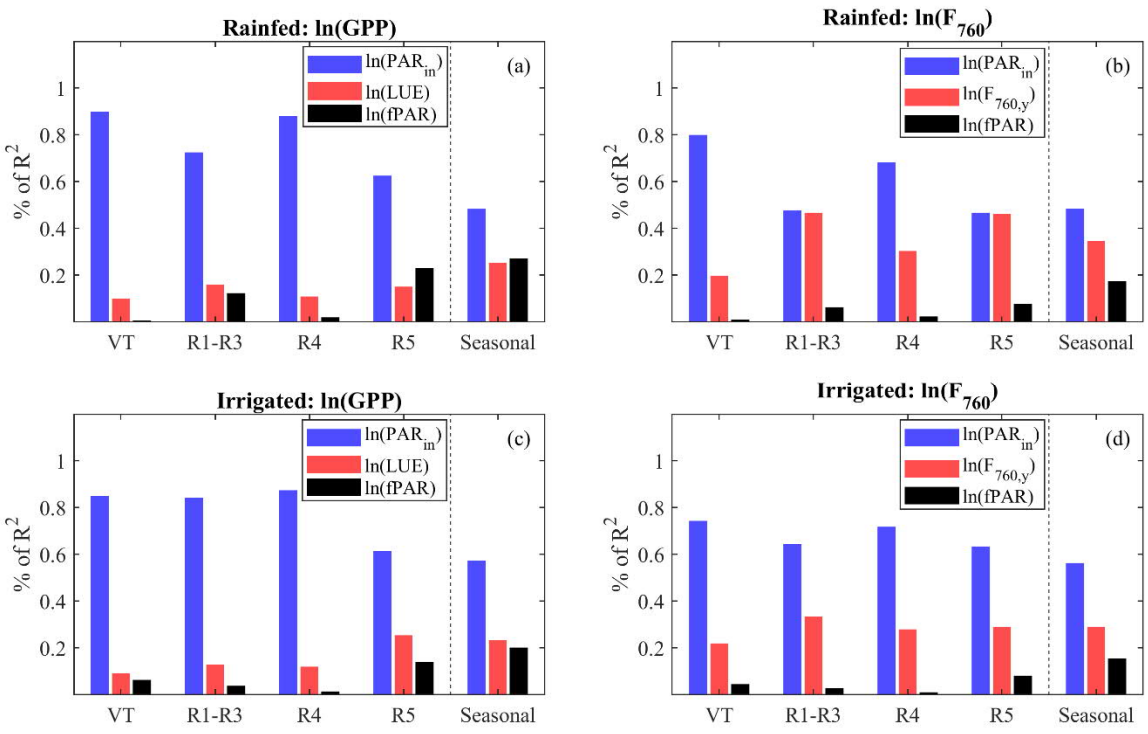

Figure S4. The relative importance metrics of natural-log-transformed PARin, $fPAR_{green}$, and $LUE/F_{760,y}$ as drivers of (a) transformed GPP and (b) transformed F_{760} at VT, R1-R3, R4, and R5 growth stages and at the seasonal scale at the rainfed maize site, and (c) transformed GPP and (d) transformed F_{760} at the irrigated maize site.

Note:

(1) $fPAR_{green}$ was calculated from Rededge-NDVI index (Rededge_NDVI = $\frac{r_{750}-r_{705}}{r_{750}+r_{705}}$, $fPAR_{green}$ = 1.37×Rededge_NDVI – 0.17, Viña & Gitelson, 2005).

(2) Rededge-NDVI index was calculated from the nadir-view reflectance measured by the HR2000+ path of the FluoSpec2 system (see section 2.2).

Table S1. Recorded five growth stages of the plants sampled from the rainfed and the irrigated maize sites in 2017 at Mead, Nebraska, and the four stages used in the current study.

Growth Stage	DOY (starting dates of each stage)		Growth stage used in this study	Time period (DOY)	
	Irrigated	Rainfed		Irrigated	Rainfed
VT	195	197	VT	196-200	196-204
R1	201	205	R1-R3	201-218	205-221
R3	208	216			
R4	219	222	R4	219-240	222-246
R5	241	247	R5	241-260	247-260

Table S2 Linear regression slope and correlation coefficients (r) of GPP:APAR, F_{760}:APAR, LUE:APAR, and $F_{760,y}$:APAR relationships

Growth stage	GPP:APAR relationship		F_{760}:APAR relationship		LUE:APAR relationship		$F_{760,y}$:APAR relationship	
	Fitted slope (p-value)	r	Fitted slope (p-value)	r	Fitted slope (p-value)	r	Fitted slope (p-value)	r
Rainfed								
VT	(3.23±0.24) $\times10^{-2}$ (<0.01)	0.8703	(1.20±0.07) $\times10^{-3}$ (<0.01)	0.8997	-(8.44±1.71) $\times10^{-6}$ (<0.01)	-0.5515	(2.87±4.31) $\times10^{-8}$ (0.51)	0.0726
R1-R3	(3.03±0.26) $\times10^{-2}$ (<0.01)	0.8197	(6.57±1.21) $\times10^{-4}$ (<0.01)	0.5458	-(7.33±1.92) $\times10^{-6}$ (<0.01)	-0.4226	(-2.69±0.80) $\times10^{-7}$ (<0.01)	-0.3748
R4	(3.18±0.15) $\times10^{-2}$ (<0.01)	0.8552	(8.88±0.57) $\times10^{-4}$ (<0.01)	0.7894	-(3.50±1.12) $\times10^{-6}$ (<0.01)	-0.2417	(-5.72±4.50) $\times10^{-8}$ (0.21)	-0.1036
R5	(1.45±0.22) $\times10^{-2}$ (<0.01)	0.6094	(8.79±0.89) $\times10^{-4}$ (<0.01)	0.7692	-(1.03±0.18) $\times10^{-5}$ (<0.01)	-0.5591	(2.03±0.73) $\times10^{-7}$ (<0.01)	0.3193
All stages	(3.71±0.18) $\times10^{-2}$ (<0.01)	0.7376	(1.20±0.05) $\times10^{-4}$ (<0.01)	0.7533	(0.61±1.37) $\times10^{-6}$ (0.65)	0.0237	(1.51±0.39) $\times10^{-7}$ (<0.01)	0.1955
Irrigated								
VT	(3.84±0.20) $\times10^{-2}$ (<0.01)	0.9139	(1.30±0.07) $\times10^{-3}$ (<0.01)	0.9004	-(5.51±1.61) $\times10^{-6}$ (<0.01)	-0.3666	(5.24±4.46) $\times 10^{-8}$ (0.24)	0.1249
R1-R3	(3.66±0.16) $\times10^{-2}$ (<0.01)	0.8867	(9.35±0.63) $\times10^{-4}$ (<0.01)	0.7649	-(4.63±1.22) $\times10^{-6}$ (<0.01)	-0.2974	(-5.73±4.35) $\times 10^{-8}$ (0.19)	-0.1046
R4	(3.45±0.13) $\times10^{-2}$ (<0.01)	0.8695	(9.55±0.54) $\times10^{-4}$ (<0.01)	0.7563	-(3.15±0.93) $\times10^{-6}$ (<0.01)	-0.2128	(-7.58±3.93) $\times 10^{-8}$ (0.055)	-0.1258
R5	(2.64±0.19) $\times10^{-2}$ (<0.01)	0.6797	(9.29±0.42) $\times10^{-4}$ (<0.01)	0.8402	-(3.82±1.64) $\times10^{-6}$ (0.02)	-0.1549	(1.02±0.37) $\times 10^{-7}$ (<0.01)	0.1896
All stages	(3.94±0.11) $\times10^{-2}$ (<0.01)	0.8035	(1.10±0.03) $\times10^{-4}$ (<0.01)	0.8098	(1.30±0.89) $\times10^{-6}$ (0.14)	0.0285	(1.23±0.24) $\times 10^{-7}$ (<0.01)	0.1876

SI References

Grömping, U. (2007). Estimators of relative importance in linear regression based on variance decomposition. The American Statistician, 61, 139–147. https://doi.org/10.1198/000313007X188252

Viña, A., & Gitelson, A. A. (2005). New developments in the remote estimation of the fraction of absorbed photosynthetically active radiation in crops. Geophysical Research Letters, 32(17), 1–4. https://doi.org/10.1029/2005GL023647